

Multidirectional Site Response Analysis of Submarine Slopes Using the Constitutive Model MSimpleDSS

T. Anantanavanich, J.M. Pestana & B.D. Carlton

University of California at Berkeley, USA



SUMMARY:

The constitutive model MSimpleDSS was implemented in the dynamic finite element program AMPLE2D. Multidirectional site response analyses were then performed to determine the effect of ground motion characteristics, depth to bedrock, initial stiffness of the soil profile, presence of an overconsolidated crust, and multidirectional shearing on the seismic response of submarine slopes. This study found that through the incorporation of multidirectional loading and rate effects, slope displacements and excess pore pressures developed at the end of shaking can be 20 to 30% higher than that under uni-directional shaking. These results suggest that current State-of-the-Practice risk analyses for submarine slopes may yield unconservative results.

Keywords: Constitutive laws, submerged slopes, multidirectional shaking, MSimpleDSS

1. INTRODUCTION

Submarine slope instability is considered to be one of the most serious threats to offshore installations such as communication cables, pipelines, production wells, and oil platforms. The magnitude of stress, strain, and excess pore pressure developed within the slope are essential elements for assessing slope performance during and after seismic events. However, most of the information on the properties of deep submarine sediments is proprietary and not readily available to the general public. In the absence of this information, numerical modeling becomes a necessary tool to understanding ground response characteristics of submarine slopes.

The constitutive model MSimpleDSS (Anantanavanich 2006), developed by the authors of this paper and described in detail in a companion paper, was implemented in an existing time-domain non-linear finite element code called AMPLE2000 (Pestana and Nadim 2000). The program was extended to accommodate multidirectional shaking and shall hereafter be referred to as AMPLE2D. AMPLE2D was validated against the equivalent linear program SHAKE for low intensity input motions. The MSimpleDSS model was specifically designed to include the anisotropic effect of the slope in the model formulation, and it allows for strain-rate adjustable parameters that can describe the rate-dependent response of soft clay, providing an accurate description of shear modulus degradation and damping ratio versus cyclic shear strain. Model parameters were estimated from laboratory tests on normally consolidated Young Bay Mud (YBM), which is representative of the medium plasticity soft clay predominantly found on the bottom of the seafloor. In this paper the MSimpleDSS model was used to investigate the effect of ground motion characteristics, depth to bedrock, initial stiffness of the soil profile, presence of an overconsolidated crust, and multidirectional shearing on the seismic response of submarine slopes.

2. SITE RESPONSE

2.1 Idealized soil profiles

The predominant soil found on continental shelves is medium to high plasticity clay (PI of 20 to 80). Monotonic and cyclic laboratory test results on offshore soil samples obtained from different locations (e.g., Chaney and Fang 1986; Houston and Herrmann 1980) have revealed that the stress-strain characteristics, strength, and pore pressure generation response are not significantly different from that of terrestrial or bay deposits since their mineralogy, plasticity, and activity characteristics are similar. Therefore, the shear wave velocity (V_s) and the small strain shear modulus (G_{max}) profile were estimated from onshore (Dickenson 1994) and offshore (Hamilton 1976a; Chaney and Fang 1986) in-situ measurements as well as laboratory results (Hardin 1978; Jamiolkowsky et al. 1991) for medium to high plasticity clays. These are shown in Figure 2.1 along with the two proposed soil profiles for this study. Profile A represents an average value of shear wave velocity while profile B has a higher initial stiffness, which represents the effect of aging. The density profile was obtained by regression analyses (Hamilton 1976b) from selected data of the Deep Sea Drilling Project (DSDP). Soil columns of 20 and 100 meters for both profile A and B were considered to determine the effect of depth to bedrock.

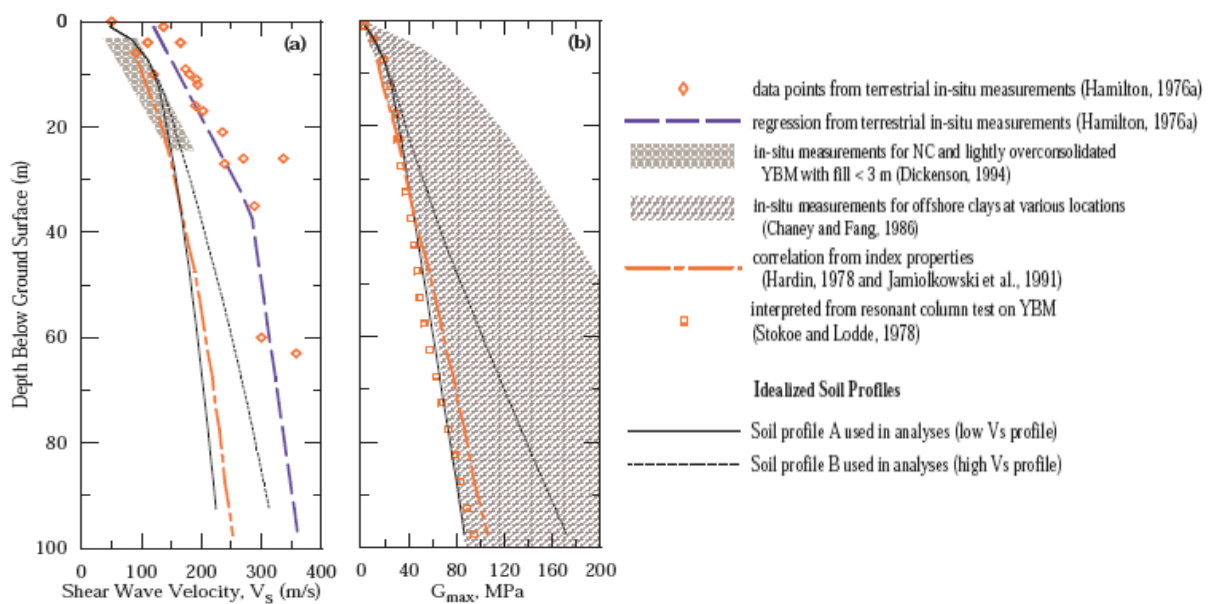


Figure 2.1. Generic soil profiles (a) shear wave velocity, (b) small strain shear modulus

2.2 Input parameters and shear modulus reduction and damping curves

The material parameters for the MSimpleDSS model were calibrated for YBM since it has similar characteristics to offshore soils and is well studied. The parameters are given in Table 2.1.

Table 2.1. MSimpleDSS model parameters for Young Bay Mud

Parameter	β	m	ψ	G_n	G_p	θ	λ
Value	0.58	12 ^a	25.5	varies ^b	270	13	180

^a varies from 12 for level ground to 16 for slope of 10 degrees

^b varies with depth, Profile A $G_n = 150$ -675, Profile B $G_n = 300$ -675

In the MSimpleDSS model, parameter G_n influences the location of modulus degradation and damping curves. Since parameter G_n varies with depth, the model predicts the modulus degradation and damping curves to be a function of depth (i.e., confining pressure dependent). This is consistent with measured data showing that, for a given shear strain, as confining pressure increases the soil behaves more linear with decreased damping. In order to obtain a better match with laboratory determined damping curves at low strain amplitude, a viscous damping matrix of 1.5% was assembled for the system in the finite element formulation of the program AMPLE2D. This additional viscous damping

matrix also suppresses noise in the solution without altering the general character of the predicted ground response (e.g., Idriss et al. 1976; Lam et al. 1978; Tsai 1980).

2.3 Input motions

The input motions used for the study are from outcropping rock sites recorded during the 1989 Loma Prieta $M_w = 6.9$ earthquake. Figure 2.2 presents the time histories of the original records and Figure 2.3 presents the acceleration response spectra with 5% damping for the original and scaled acceleration time series.

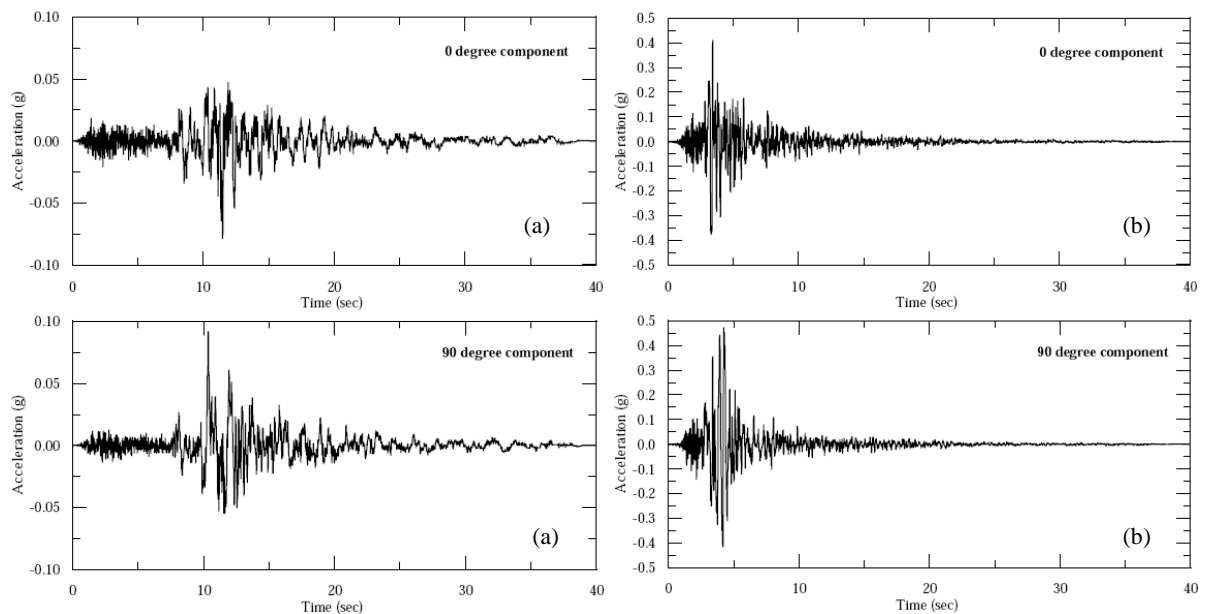


Figure 2.2. Acceleration time histories of the original input motions, 1989 Loma Prieta Earthquake, $M_w = 6.9$, a) Rincon Hill Station, $R_{rup} = 79.7$ km. b) Gilroy Array #1 Station, $R_{rup} = 11.2$ km.

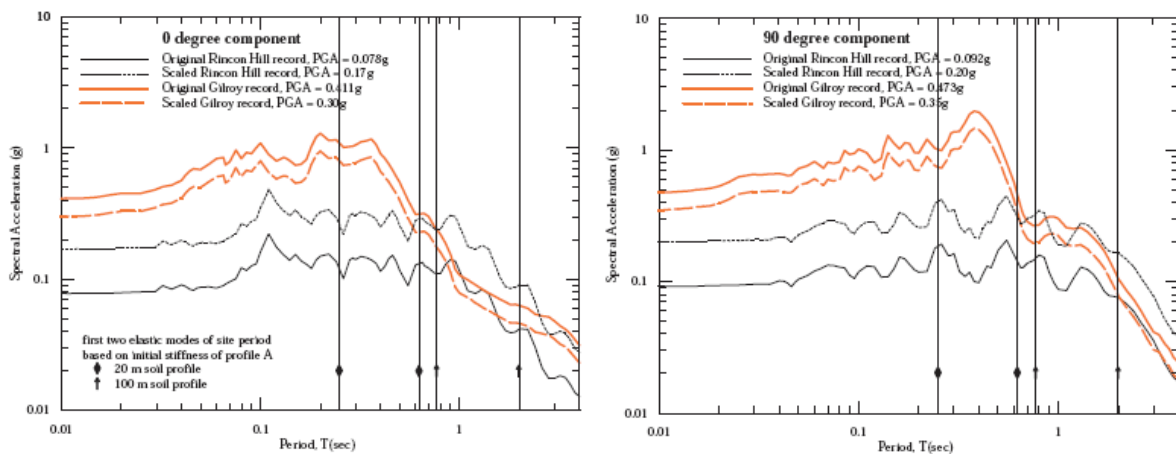


Figure 2.3. Acceleration response spectra of selected bedrock input ground motions from the 1989 Loma Prieta earthquake shown in log scale.

The first set of motions are from Rincon Hill, which is 79.7km from the fault rupture, with PGA of 0.078 and 0.092 g for the 0 and 90 degree components, respectively. The second set of motions are from Gilroy (CA) Array #1, which is 11.2 km from the fault rupture, with PGA of 0.411 and 0.473 g for the 0 and 90 degree components, respectively. These two records were chosen due to the large difference in frequency contents. Each of the two ground motions was also scaled to investigate the effect of earthquake amplitude. The Rincon Hill records were scaled to PGA of 0.17 and 0.20 g for

the 0 and 90 degree components, respectively, and the Gilroy records were scaled to PGA of 0.30 and 0.35 g for the 0 and 90 degree components, respectively.

3. RESULTS

3.2 Effect of ground motion characteristics

In order to separate the multidirectional effects from ground motion characteristics, analyses in this section were performed using nonlinear 1-D analysis. Examination between responses from original and scaled input motions reveals that higher intensity motions result in larger shear strain and nonlinear behavior. As expected, the response spectra at the ground surface of the stronger input motions have higher amplitude at small frequencies. These differences decrease as the frequency increases. Therefore, as the site increases its nonlinearity, there is a loss of high frequency spectral peaks which results in an effective transfer of energy from higher to lower frequencies. The same conclusion was found from nonlinear site response analyses of soft and deep cohesive soil sites by Lam et al. (1978), Tsai (1980), Dickenson (1994), and Seed and Dickenson (1995).

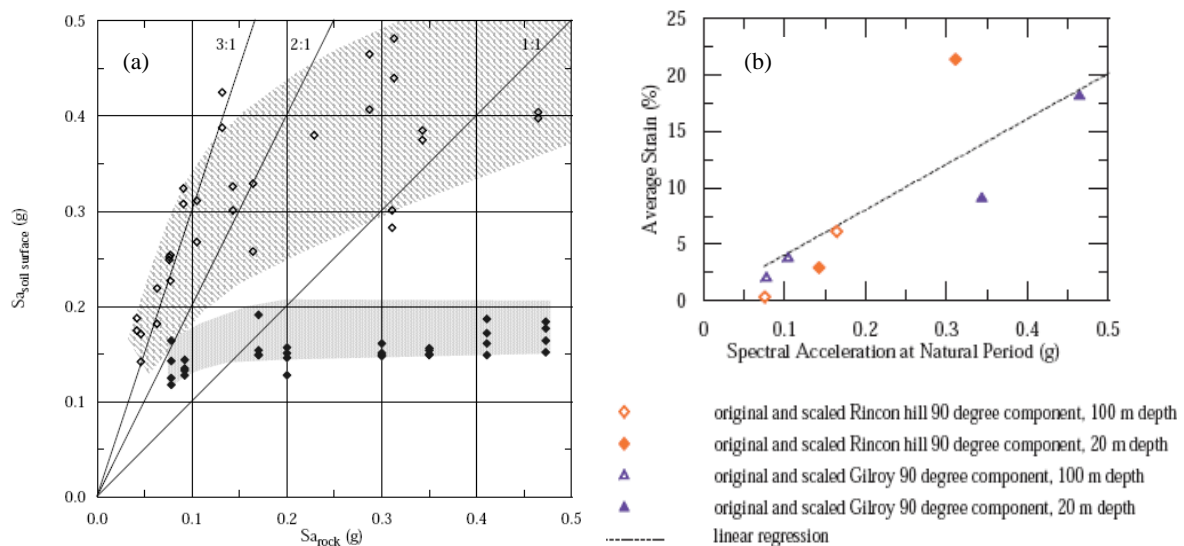


Figure 3.1. a) AMPLE2D predictions of the relationships between PGA_{rock} (closed diamonds), $Sa_{rock}(T_o)$ (open diamonds), and $Sa_{surface}(T_o)$. b) Correlation between average strain and spectral acceleration at natural site period of input motions. All were on 10° slope using 1-D analyses from AMPLE2D.

Figure 3.1a compares the relationship between the spectral acceleration at the natural site period at the surface ($Sa_{surface}(T_o)$) with the spectral acceleration at the natural site period at bedrock ($Sa_{rock}(T_o)$) and the PGA at bedrock (PGA_{rock}). From Figure 3.1a, it is apparent that the ratio of $Sa_{surface}(T_o)/Sa_{rock}(T_o)$ is around 3 for $Sa_{rock}(T_o) < 0.1$ g and decreases to 1 at $Sa_{rock}(T_o) \sim 0.45$ g. As the intensity of the motion increases the intensity at the ground surface also increases, but only when comparing spectral acceleration at the natural site period. Soil nonlinearity has a much greater effect when comparing PGA_{rock} with $PGA_{surface}$ or $Sa_{surface}(T_o)$, and the response remains almost the same for all input PGA.

Figure 3.1b presents the relationship of the average shear strain that the soil profiles experience with the spectral acceleration at the site period for each input motion. These average shear strains, which are index parameters that represent degree of slope damage, were computed by dividing the displacement at the ground surface by 20% of the thickness of each soil profile where most of the shear strains were developed. This normalizing procedure allows the response of soil profiles with different thicknesses to be plotted in the same figure. From Figure 3.1b one can see that there is a good correlation between $Sa_{surface}(T_o)$ and slope damage as defined by the average shear strain.

3.3 Effect of depth of bedrock

The effect of depth of bedrock on the response of sloping ground sites was analyzed using a 10 degree slope. As expected, the simulations showed that the predominant period of the ground surface response increased as the thickness increased. This is due to the fact that the high frequency content is more filtered out, giving deeper soil profiles higher spectral amplitude at long periods and lower spectral amplitude at short periods. Hence, the response of the structure at a site much depends on its structural period and the assumption of the thickness of the soil profile.

3.4 Effect of initial stiffness of soil profile

The effects of initial stiffness on the response of sloping ground are illustrated in Figure 3.2, which shows displacement, shear strain, and excess pore pressure developed at the end of shaking. Two components of each earthquake were applied simultaneously to the soil profile with the 90 degree component acting in the dip direction, and the 0 degree component in the strike direction. The results from model simulations reveal that the responses of soil profiles under sloping ground condition are not very sensitive to the initial stiffness of the soil profile.

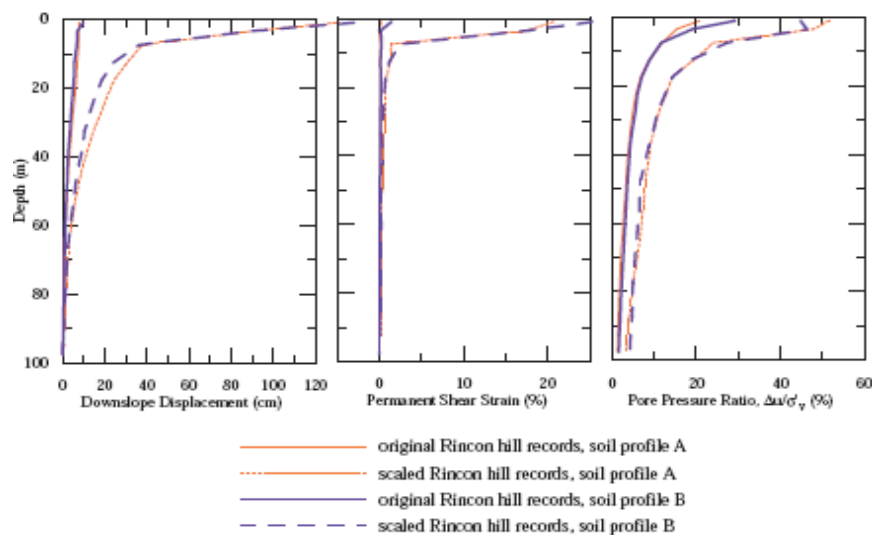


Figure 3.2: Effect of initial stiffness of soil profile on permanent displacements, permanent strain, and pore pressure ratio for 100 meter soil profile A and B with slope inclination of 10°, 2-D analyses from AMPLE2D.

3.5 Effect of overconsolidated crust

The upper layers of soil deposits in the submarine environment are frequently overconsolidated, creating a crust type profile. Crust profiles are associated with higher shear strength in the upper layers and an abrupt decrease of strength below the crust. Parametric studies suggest that crusts have a noticeable effect on ground surface response spectra (Lam et al. 1978; Tsai 1980). For the problem of submarine slope instability, Bea and Arnold (1973) performed nonlinear finite element analysis of an infinite slope subjected to wave-induced shear stress from storm loading. They found that the existence of an overconsolidated crust has a detrimental effect on slope stability because it creates a weak layer directly beneath the crust. The weak layer could entrap seismic energy, causing significant shear strain and large amounts of pore pressure generation, which could initiate slope instability and lead to catastrophic failure.

To determine the effects of a crust on the dynamic response of submarine slopes, analyses were performed on an additional idealized soil profile with an overconsolidated crust in the top 20 m. The crust type profile was subjected to the scaled 90 degree component of the Rincon Hill record. The results are plotted in Figure 3.3 along with the response from a normally consolidated soil profile with no crust. Since energy is concentrated at the bottom of the crust, higher displacements, shear strains,

and pore pressures are developed in this weak layer compared to that of the normally consolidated soil profile. The failure is likely to initiate at this layer and the relatively undisturbed soils in the crust will essentially slide on top of it. The sliding effect of the stiffer crust layer is more likely to cause tsunamis than the failure of normally consolidated soils since the stiffer soils will effectively slide as a rigid block (Tappin et al. 2001).

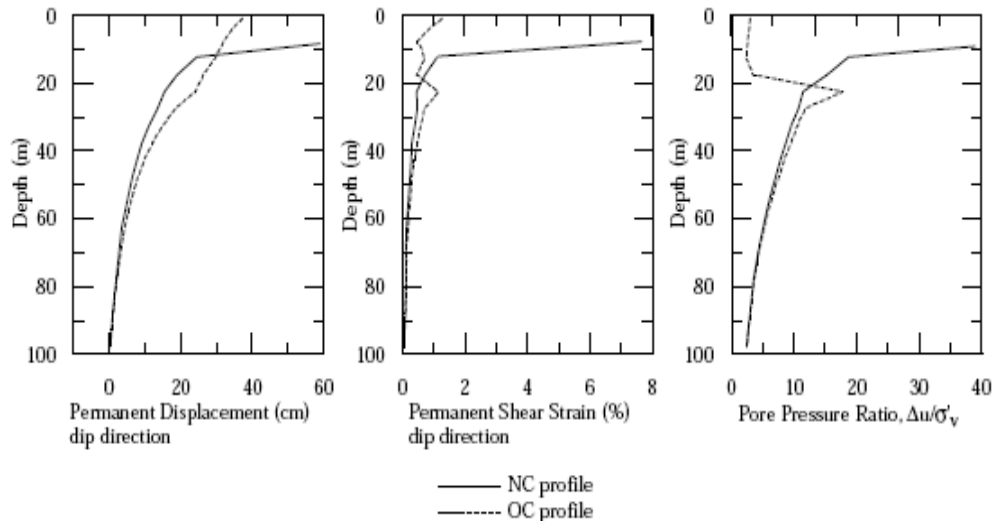


Figure 3.3. Effect of overconsolidated crust on displacement, shear strain, and pore pressure for 100 meter soil profile with slope inclination of 10° subjected to the scaled Rincon Hill record, 1-D analysis from AMPLE2D.

3.6 Effect of multidirectional shaking

As indicated from extensive laboratory stress-controlled cyclic tests on granular soil (e.g., Pyke et al. 1975; Ishihara and Nagase 1985; Kammerer et al. 2003), soil response under multidirectional shearing tends to generate pore pressure faster than that of unidirectional shearing at the same magnitude. The 100 and 20m soil profiles with slope inclinations of 5 and 10 degrees were subjected to the original and scaled input motions under both unidirectional and multidirectional shaking. The orientation was arbitrarily chosen such that the 90 degree component was acting in the dip direction and the 0 degree component was acting in the strike direction. The one-directional analyses were performed by applying the 90 degree component in the dip direction.

The influence of multidirectional shearing on accumulated displacement at the end of shaking is shown in Figure 3.4 for the 100 and 20m soil profiles under a slope inclination of 10 degrees. The effect of multidirectional shearing on displacement is expressed in terms of the multidirectional displacement ratio (MDR), which is the percent increase in displacement accumulated under multidirectional shaking over that of one-directional shaking at a given depth. Results from the analyses show that for the 100m soil profile the one-directional analyses can underestimate the displacement at the ground surface on the average of 20%. For the shallower 20m soil profile, the multidirectional shaking analyses predict about 40 to 60% more displacement.

The influence of multidirectional shearing on pore pressure generation is shown in Figure 3.5 for 20m soil profiles under slope inclinations of 0, 5, and 10 degrees. The effect of multidirectional shearing on pore pressure generation is expressed in terms of the multidirectional pore pressure ratio (MPR), which is the percent increase in the magnitude of pore pressure developed under multidirectional shaking over that of one-directional shaking. In general, the analyses suggest that the average MPR is in the order of 20 to 30%. This value tends to increase as the slope inclination increases and/or the thickness of the soil profile decreases. It can be seen that vibration-type motions such as the Rincon Hill records produce higher values of MPR than that of shock-type motions such as the Gilroy records.

This finding is confirmed by experimental results obtained from centrifuge tests on the free field response of level saturated sand deposits subjected to both unidirectional and multidirectional shaking (Su and Li 2003). Su and Li found that the maximum pore pressure at great depths for multidirectional shaking was about 20% larger than that in one-directional shaking and the difference reduced to about 10% near the surface.

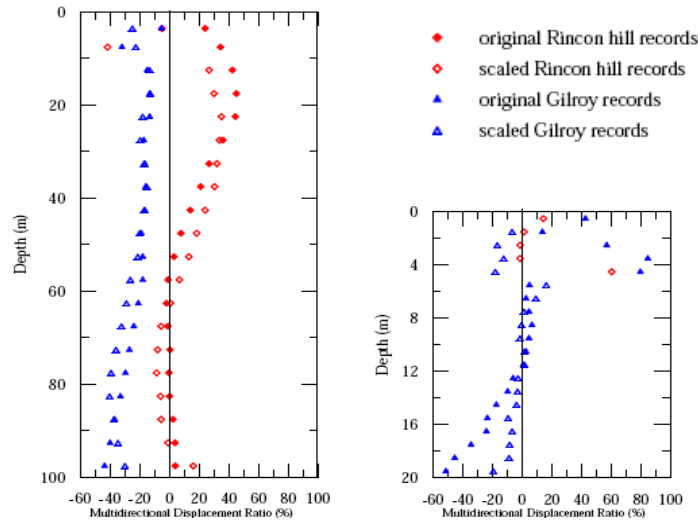


Figure 3.4. Variation of multidirectional displacement ratio (MDR), $(D_{2D}-D_{1D})/D_{1D}$, with depth for 100 and 20m soil profile under 10° slope inclination subjected to the selected input motions, AMPLE2D predictions

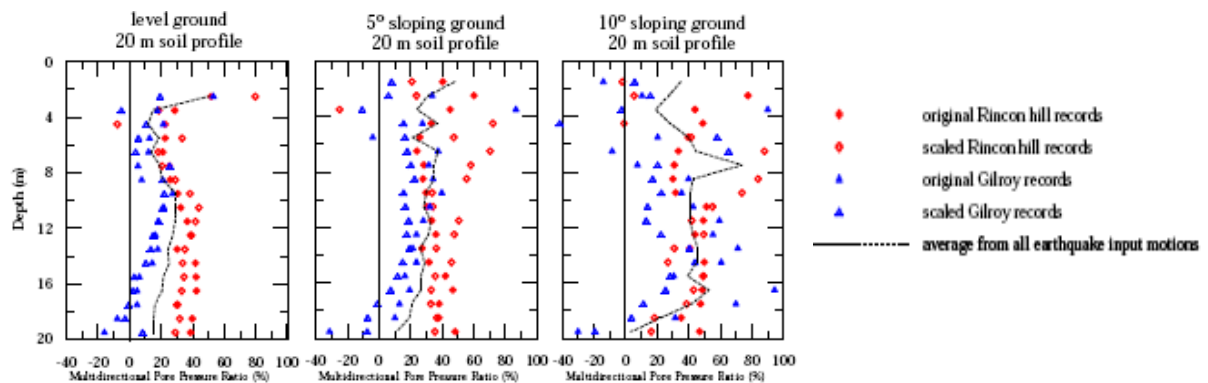


Figure 3.5. Variation of multidirectional pore pressure ratio (MPR), $(\Delta u_{2D} - \Delta u_{1D})/\Delta u_{1D}$, with depth for 100 and 20 meter depth under level ground, 5, and 10° slope inclination

The potential for slope failure due to pore pressure redistribution and undrained creep phenomena sometime after the end of shaking is highly dependent on the amount of pore pressure generated during shaking. Therefore, any additional pore pressure generation due to motion in a second direction should not be disregarded. Results of the above analyses have shown that the impact of multidirectional shaking on pore pressure generation is primarily due to the additional shaking amplitude from the motion in the second direction, whereas the impact of variation of shearing direction is of secondary importance.

4. PERFORMANCE OF SUBMARINE SLOPES

To validate results from model simulations, the displacements computed at the ground surface for different slope inclinations and soil thicknesses were compared with Makdisi and Seed (1978), and Bray et al. (1998). These simplified procedures are appropriate for the case where there is no significant strength loss or large pore pressure build up. Therefore, validation was done by evaluating

results from the cases that have no significant pore pressure generation. The values of yield acceleration ratio (k_y/k_{max}) obtained from the simplified procedures together with the permanent displacement computed at the ground surface using AMPLE2D were plotted for 100 and 20m deep soil profiles with slope inclinations at 2.5, 5, 7.5, and 10° in Figure 4.1, along with the variation of permanent displacement with yield acceleration ratio for earthquakes with an $M_w = 7$ proposed by Makdisi and Seed (1978) and Bray et al. (1998). The scattered data and the mean values from AMPLE2D analyses are in excellent agreement with the simplified procedures.

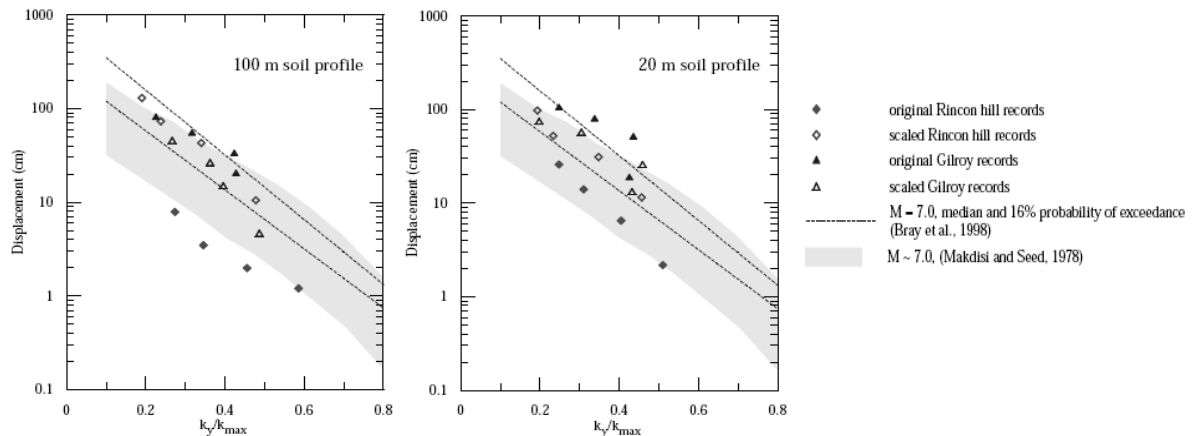


Figure 4.1. Model predictions on the variation of permanent displacement as a function of yield acceleration for 100 and 20 meter soil profile with 2.5, 5, 7.5, and 10° slope inclination.

Although the slope might not fail during the earthquake, significant excess pore pressures generated during shaking could initiate slope failure due to redistribution of pore pressure some time after the end of shaking (Biscontin 2001). The time required for slope failure depends on the magnitude and combination of hydraulic conductivity at each soil depth. Therefore, the magnitude of pore pressure developed at the end of shaking could serve as an important index in the assessment of post-seismic stability. The failure susceptibility, defined here as Failure Triggering Index ($FTI = \Delta u / \Delta u_{max}$), can be estimated in terms of the ratio between the magnitude of pore pressure ratio developed at the end of undrained loading to the pore pressure ratio at failure. For the present study on NC YBM, a minimum value of FTI of about 75 to 80% is assumed to initiate slope failure. From results of all numerical simulations, it was consistently found that when FTI reached this threshold value, the yield acceleration ratio (k_y/k_{max}) was usually less than 0.25 to 0.20. At this threshold value, soil profiles start to develop significant shear strains and generate large amounts of pore pressure.

The corresponding yield acceleration ratio, k_y/k_{max} , can be computed for a selected combination of undrained shear strength, slope inclination, and intensity of input ground motion. By calculating the value of k_y/k_{max} under various combinations, the relationship between k_y/k_{max} , PGA of bedrock motion, and slope inclination can be developed. The boundary that separates the condition of slope failure can be estimated based on the k_y/k_{max} threshold value of 0.20 to 0.25. Figure 4.2 illustrates such boundaries developed for normally consolidated Young Bay Mud and Boston Blue Clay for shallow failures.

To compare the results of the simplified procedure with those from nonlinear model predictions, Figure 4.3 was created with results from AMPLE2D predictions that show the variation of FTI. It can be seen that the boundary from the simplified k_y/k_{max} given in Figure 4.2 matches well with results from the nonlinear AMPLE2D analyses in Figure 4.3. The degree of slope damage was found to correlate better with spectral acceleration at site period rather than the PGA of input ground motion. It should be pointed out that the combinations that are located outside the failure zone do not necessarily mean that the possibility of slope failure is zero. Although the FTI index is less than about 75 to 80% outside the failure zone, the redistribution of excess pore pressure is still important for post-earthquake slope stability.

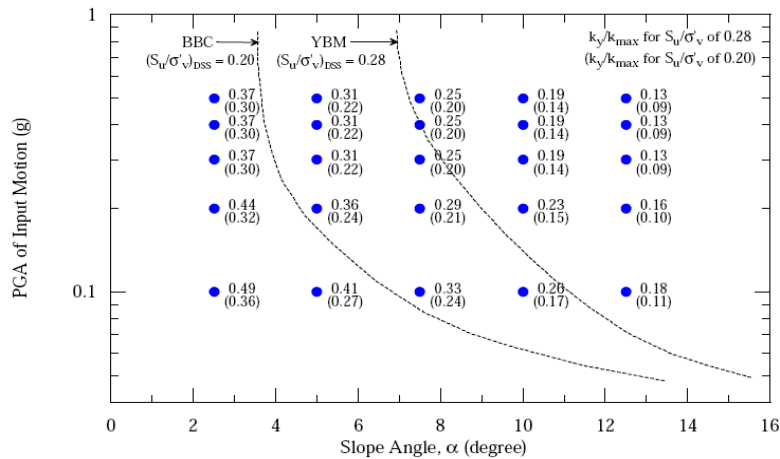


Figure 4.2. Variation of slope failure with slope angle and PGA of input motions for NC Young Bay Mud (medium to high plasticity) and Boston Blue Clay (low plasticity) using simplified k_y/k_{max} method.

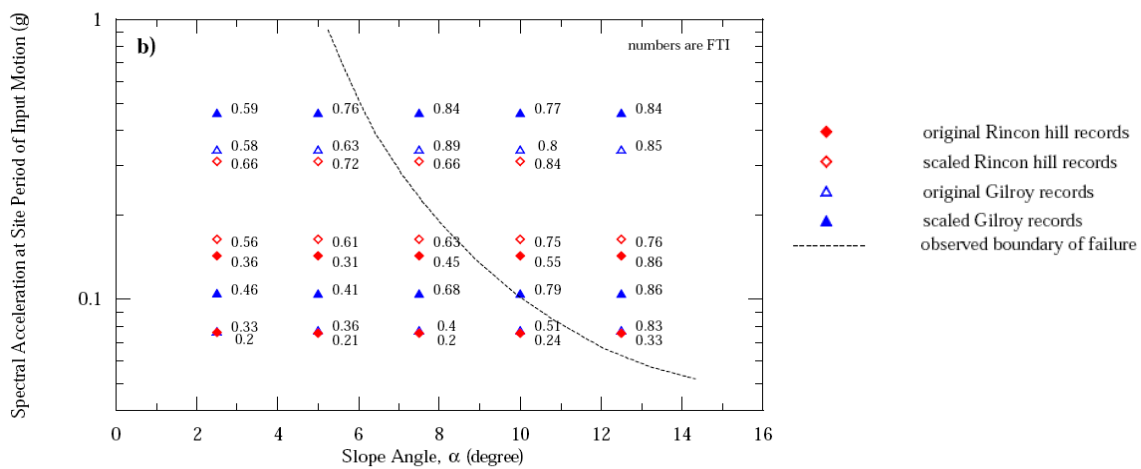


Figure 4.3. Model simulations of the variation of FTI with slope angle and spectral acceleration at the initial site period for 100 and 20 meter NC YBM profile subjected to the selected input motions.

5. CONCLUSION

The MSimpleDSS model was implemented in the finite element program AMPLE2D and used to predict the behavior of submerged slopes of soft soil deposits subjected to seismic loading. Based on the results it can be concluded that:

The model predicts amplification of PGA below a maximum value, above which the surface PGA remains unchanged due to soil nonlinearity. The magnitude of spectral acceleration at the initial site period correlates better with the degree of slope damage than the PGA of the input motion.

The depth to bedrock changes the initial site period, therefore the response of the structure at a site depends on its structural period and the assumption of the thickness of the soil profile. The displacement, shear strain, and pore pressure generation for sloping ground conditions are not very sensitive to the initial stiffness of the soil profile. Soil profiles with overconsolidated crusts trap energy at the weak layer just beneath the crust, increasing shear strains and pore pressures, which make it more susceptible to failure. Soil profiles with crusts are more likely to cause tsunamis when they fail because they fail as a rigid block.

Results from multidirectional shaking predict slope displacements on average 20% greater and generated excess pore pressures about 20-30% more than predictions from unidirectional analyses. Therefore, unidirectional site response analyses could give unconservative results.

The failure susceptibility, defined as the Failure Triggering Index ($FTI = \Delta u / \Delta u_{max}$), was proposed as an index to identify the potential of failure due to the generated pore pressure. By using the threshold value of FTI as the criteria in defining the initiation of slope failure, a simplified procedure was proposed to evaluate the post-seismic stability for various degrees of slope inclinations, earthquake intensities, and soil types. This procedure incorporates the nonlinear behavior of soil and includes calibrations with the predicted performance of the slope by the nonlinear analysis.

ACKNOWLEDGEMENTS

This work was sponsored by the United States National Science Foundation.

REFERENCES

- Anantanavanich, T. (2006). *Modeling the rate dependent dynamic response of submarine soft clay deposits*. Ph. D. thesis, Department of Civil and Environmental Engineering, UC Berkeley.
- Bea, R. and P. Arnold (1973). Movements and forces developed by wave-induced slides in soft clays. In *Proceedings of the 1973 Offshore Technology Conference*, Volume II, Houston, TX.
- Biscontin, G. (2001). *Modeling the Dynamic Behavior of Lightly Overconsolidated Soil Deposits on Submerged Slopes*. Ph. D. thesis, Department of Civil and Environmental Engineering, UC Berkeley.
- Bray, J., E. Rathje, A. Augello, and S. Merry (1998). Simplified seismic design procedure for lined solid-waste landfills. *Geosynthetics International Journal* 5 (1-2), 203-235.
- Chaney, R. C. and H. Y. Fang (1986). Static and dynamic properties of marine sediments: A State of the Art. In *Marine Geotechnology and Nearshore/Offshore Structures*, Philadelphia.
- Dickenson, S. (1994). *Dynamic Response Analyses of Deep and Soft Cohesive Soil Site*. Ph. D. thesis, Department of Civil and Environmental Engineering, UC Berkeley.
- Hamilton, E. L. (1976a). Shear-wave velocity versus depth in marine sediments: A review. *Geophysics* 41 (5), 985-996.
- Hamilton, E. L. (1976b). Variations of density and porosity with depth in deep-sea sediments. *Journal of Sedimentary Petrology* 46 (2), 280-300.
- Hardin, B. (1978). The nature of stress-strain behavior of soils. In *Proceedings of the Special Conference on Earthquake Engineering and Soil Dynamics*, Volume 1, Pasadena, California, pp. 3-89. ASCE.
- Houston, W. N. and H. G. Herrmann (1980). Undrained cyclic strength of marine soil. *Journal of Geotechnical Engineering Division* 106 (GT6), 691-712.
- Idriss, I., R. Dobry, E. Doyle, and R. Singh (1976). Behavior of soft clays under earthquake loading conditions. In *Proceedings, Offshore Technology Conference*, Volume III.
- Ishihara, K. and H. Nagase (1985). Multi-directional irregular loading tests on sand. In *Advances in the Art of Testing Soils Under Cyclic Conditions*, Detroit, Michigan, pp. 99-119.
- Jamiolkowsky, M., S. Leroueil, and D. LoPresti (1991). Theme lecture: Design parameters from theory to practice. In *Proceedings of the Geo-Coast 1991*, Yokohama, Japan, pp. 1-41.
- Kammerer, A., J. Pestana, and R. Seed (2003). Behavior of Monterey 0/30 sand under multidirectional loading conditions. In *Geomechanics: Testing, Modeling, and Simulation*, GSP 143.
- Lam, I., C. F. Tsai, and G. R. Martin (1978). Determination of site dependent spectra using nonlinear analysis. In *Second International Conference on Microzonation*, San Francisco, California, pp. 1089-1104.
- Makdisi, F. and H. Seed (1978). Simplified procedure for estimating dam and embankment earthquake-induced deformations. *Journal of Geotechnical Engineering Division* 104 (GT7), 849-867.
- Pestana, J., G. Biscontin, F. Nadim, and K. Andersen (2000). Modeling cyclic behavior of lightly overconsolidated clays in simple shear. *Soil Dynamics and Earthquake Engineering* 19, 501-519.
- Pyke, R. M., H. Seed, and C. K. Chan (1975). Settlement of sands under multidirectional shaking. *Journal of Geotechnical Engineering Division* 101 (GT4), 379-398.
- Seed, R. and S. Dickenson (1995). Site-dependent seismic site response. In *Second International Workshop on Wind and Earthquake Engineering for Offshore and Coastal Facilities*, Berkeley, CA.
- Su, D. and X. Li (2003). Centrifuge tests on earthquake response of sand deposit subjected to multi-directional shaking. In *The 16th ASCE Engineering Mechanics Conference*, University of Washington, Seattle. ASCE.
- Tappin, D., P. Watts, G. McMurtry, Y. Lafoy, and T. Matsumoto (2001). The Sissano, Papua New Guinea tsunami of July 1998, offshore evidence on the source mechanism. *Marine Geology* 175, 1-23.
- Tsai, C-H., L. I. M. G. R. (1980). Seismic response of cohesive marine soils. *Journal of Geotechnical Engineering Division* 106 (GT9), 997-1012.